

# Green synthesis of Zinc Oxide nanoparticles, antibacterial studies and investigation as catalyst for the conversion of pumpkin oil into biodiesel

Rudreshappa G.E.<sup>1,2\*</sup>, Sreenivasa S.<sup>1,3</sup>, Uma K.<sup>4</sup>, Manjunatha S.<sup>5</sup> and Aruna Kumar D.B.<sup>1\*</sup>

1. Department of Studies and Research in Chemistry, Tumkur University, Tumakuru, INDIA

2. Department of Chemistry, UVCE, Bangalore, INDIA

3. Deputy Adviser, National Assessment and Accreditation Council (NAAC), Bangalore, INDIA

4. Department of Chemistry, Siddaganga Institute of Technology, Tumakuru, INDIA

5. BMS College of Engineering, Bangalore, INDIA

\*ger@sit.ac.in; nirmaldb@rediffmail.com

## Abstract

Zinc oxide nanoparticles were synthesized by employing solution combustion method using environmental friendly *Cellophylum innophyllum* seed powder as fuel. Phase purity, crystallite size were determined from X-ray diffraction (XRD). Organic species attached to the surface of the nanoparticle were identified using Fourier transform infrared spectroscopy (FTIR). Morphological studies were performed using TEM and SEM.

Bandgap increased with decreasing particle size as confirmed from the diffuse reflectance spectroscopy (DRS) white light luminescence capabilities of ZnO NPs were studied using photoluminescence spectroscopy. In vitro antibacterial activity studies and catalytic property for the conversion of pumpkin seed oil into biodiesel were performed.

**Keywords:** ZnO, *Cellophylum innophyllum*, XRD, DRS, Photo Luminescence, Biodiesel.

## Introduction

Metal oxides play a very important role in many areas of chemistry, physics and material science and even to some extent in biological applications. They are proved to be promising materials for a variety of practical applications due to their unique and tuneable properties such as optical, optoelectronic, magnetic, electrical, mechanical, thermal, catalytic, photochemical etc.<sup>27,36</sup>

Thereby, they become convenient for use in fuel cells, secondary battery materials, sensors, solar cells, super capacitors. During recent days, worldwide transportation sector is almost entirely dependent on petroleum derived fuels. Unfortunately, petroleum based products are one of the main causes of anthropogenic carbon dioxide emission to the atmosphere<sup>25,28</sup>.

CO<sub>2</sub> emission-free fuels such as sustainable and renewable energies are of great importance to meet the growing demand in domestic and commercial transportation. Biodiesel is one of the greener alternatives for fossil fuels, biodiesel generation requires catalysts. Metal oxides have shown promising results. Metal oxide nanostructures are

among the most versatile groups of semiconductor nanostructures that stand out as one of the most common, most diverse and the richest class of materials due to their interesting electronic structures, physical/chemical properties and functionalities. These materials display the most fascinating and widest range of properties<sup>1</sup>.

ZnO nanoparticles were synthesized by sol-gel combustion, CVD, sonochemical, hydrothermal, wet polymerization, solvothermal, thermal decomposition, microwave assisted precipitation, micro emulsion, lyophilisation and laser ablation. The green synthetic method employing biological plant extracts is one of the more extensively acknowledged routines due to its several advantages like no additional chemicals, simple, environmental friendly inexpensive and reliable method.

Therefore, the current investigation endeavours to synthesize ZnO nanocomposite via onestep solution combustion method by employing the *Cellophylum innophyllum* seed powder as fuel<sup>4</sup>. Cucumis melo fruit is having reasonably high contents of carbohydrates, carotenoids, vitamin A, vitamin B, vitamin C, proteins, niacin etc.<sup>19</sup> The phytochemical reviews unveil that it is consisting of plenty of polyphenols with antioxidant activity, anti-ulcer activity, anticancer activity etc. Most of these substances existing in the muskmelon juice are antioxidants and best owed with reducing nature. Consequently, they serve as reliable fuels for the preparation of metal oxide nanoparticles from metal nitrates by reduction.

Further, the synthesized nanoparticles were explored for comparative study of photocatalytic activity for hydrogen generation via water splitting using solar energy, methylene blue (MB) dye degradation, photoluminescence, electrochemical sensing of nitrite and antibacterial studies activities.<sup>5,9,11,12,14,18,20,23,24,26,32,38,40</sup>

## Material and Methods

### Synthesis:

**(a) Preparation of fuel from *Cellophylum innophyllum* seeds:** Fresh *Cellophylum innophyllum* seeds were collected and washed several times with tap water followed by distilled water. They are shade dried for two days at room temperature and then powdered using blender. The resulting powder is used for synthesis of ZnONPs.

**(b) Synthesis of ZnO nanoparticles:** 1.0 g of zinc nitrate hexahydrate  $Zn(NO_3)_2 \cdot 6H_2O$  and 80 mg of finely powdered *Cellophylum innophyllum* seeds were added to 20 mL of distilled water in a beaker and transferred into a silica crucible. The crucible was placed in a pre-heated Muffle furnace at 500 °C for ten minutes. The crucible was taken out from the Muffle furnace and kept in air for 10 minutes. Again the crucible was placed in the Muffle furnace for calcinations at 500 °C for 3 hours and allowed to cool. The same procedure was repeated with 60 mg of fine powder of *Cellophylum innophyllum* seed as fuel. The overall reaction can be represented as follows:



**(c) Basic Characterization:** The samples were characterized using powder X-ray diffractometer (Rigaku smart lab X-ray diffractometer using copper radiation with Ni filter). X-Ray diffraction at 40 kV was used to estimate the crystallite sizes. The XRD pattern was scanned from 10-80 degrees using Cu  $K\alpha$  radiation. Metal oxide bond stretching frequencies were analysed by FTIR spectrometer (Bruker-alpha). The UV measurements on the samples were measured using UV-Visible absorbance and reflectance spectrophotometers (Agilent Cary-60 and LABINDIA UV3092 spectrophotometer). The morphologies of the prepared ZnO were scanned using Scanning electron microscopy (Hitachi-7000 Table top).

Electron diffraction rings and HRTEM of the ZnO crystallites were obtained using transmission electron microscopy (TEM) attached with EDX present at the SAIF-STIC facility, Cochin (JEOL3010). Photoluminescence studies were recorded using fluorescence spectrophotometer (Agilent Cary Eclipse fluorescence spectrometer) using Xe lamp with an excitation wavelength of 398 nm.

**(d) Surface area studies:** Surface area was measured using BELSORP-mini, Japan BET surface area analyser. Nitrogen gas was used as the adsorption and desorption medium by the known quantity of the sample in a constrained volume cell.

**(e) Photocatalytic activity:** The photocatalytic activity of the synthesized cerium oxide NPs was evaluated by degradation of methylene blue (MB) in an aqueous solution at room temperature using 120 W mercury lamp as radiation source. In the typical procedure, 50-200 mg of photo catalyst was added to 100 mL of methylene blue solutions of different concentrations (5-20 ppm) in a 150 x75 mm sized batch reactor. The gap between the radiation source and the reactor was 18 cm. The solution was continuously stirred in the dark chamber for about 30 minutes to ensure the complete organization of an adsorption as well as the desorption equilibrium between the MB dye and photo catalyst. Then, 2 mL volume of the suspension was withdrawn from the above solution at a regular sequence of 30 minutes intervals.

After the removal of the photo catalyst from the solution by centrifugation, the concentration of left over aqueous solution was monitored using UV-Vis spectrophotometer at a fixed wavelength of 664 nm and the % degradation of the MB has been calculated based on the principle of Beer Lambert law .

**(f) Dye degradation studies:** Presence of organic matter (dye related) in waste water is a serious problem and their presence releases toxic substances into water that are dangerous to all living organisms either on the earth or in water. So eradication of tracer amounts of dye related materials is essential. In order to do this, four techniques and processes are available. They are physical, chemical, photocatalytic degradation, electrochemical and biological processes. Out of all the techniques and processes, the photocatalytic degradation under UV/Sun light is considered to be the best because of simplicity, time saving and cost effectiveness.

**(g) Photoluminescence studies:** Photoluminescence studies are aimed at determining the effectiveness of trapping, migration and transfer of charge carriers and to understand the fate of  $-e - h+$  pairs in semiconductors. The present study was used to understand the optical properties, surface states, oxygen vacancy and defects of ZnO NPs.

**(h) Biodiesel production using ZnO NPs and Pumpkin seeds oil:** The free fatty acid present in the pumpkin oil was determined and it was found to be 2%. Hence, single stage base transesterification was much suitable for pumpkin oil methyl ester/biodiesel production. 200g of oil was taken in a three neck round bottom flask equipped with condenser and placed on a mechanical stirrer. Initially, oil was preheated at 60 °C, then 1.5wt.% of ZnO NPs and 12:1 methanol to oil molar ratio mixture was added to the oil.

Then the reaction was carried out for a period of 90 min with temperature of 65 °C maintaining a speed of reaction at 650 rpm. After completion of the reaction, three phases are obtained: upper phase (biodiesel), middle phase (glycerine) and lower phase (catalyst). Finally, biodiesel was separated.

**(i) Antibacterial property:** Evaluation was studied by disc diffusion method, using *Escherichia coli*, *Staphylococcus aureus* and *Pseudomonas aeruginosa* in presence of nanoparticles. The zone of inhibition in mm was used to quantify the antibacterial activity.

#### Characterization

**ZnO –UV Studies:** UV-Visible spectra of zinc oxide (ZnO) nanoparticles were evaluated using optical response and the result is presented in the figure 1. The absorbance spectrum was recorded for the nanoparticles dispersed in water.

The UV-Vis spectra reveal a strong absorption band at 380 nm with a band gap of 3.26eV indicating the formation of zinc oxide (ZnO) nanoparticles<sup>41</sup>.

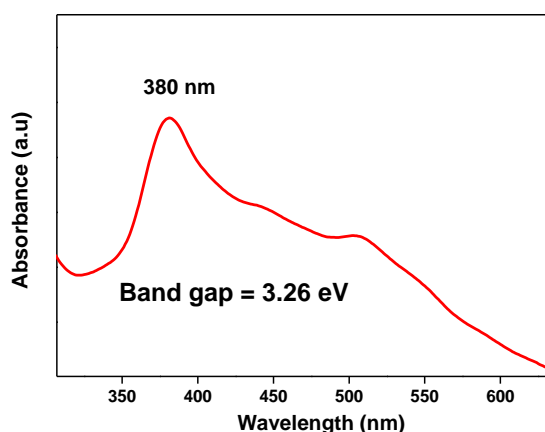


Fig. 1: UV spectrum of ZnO nanoparticles

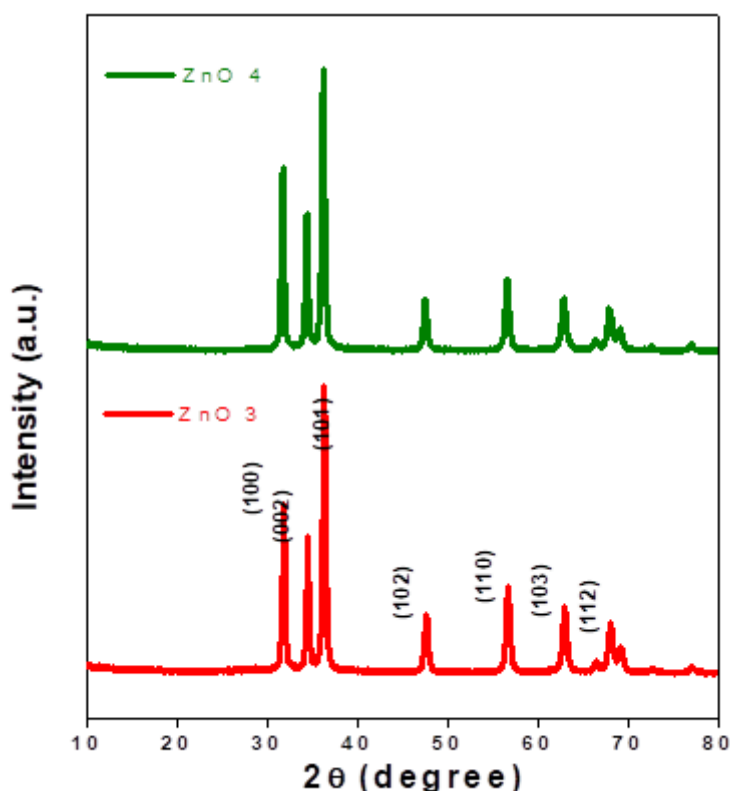


Fig. 2: XRD patterns of ZnO Nanoparticles synthesized taking 1.0g of Zinc nitrate hexahydrate  $Zn(NO_3)_2 \cdot 6H_2O$  and 80 mg and 60mg of fine powder

**ZnO - XRD Studies (PXRD):** Space group - P63 mc, structure - Hexagonal, wurtzite with an average crystalline size  $a = b = 3.249 \text{ \AA}$ ,  $c = 5.204 \text{ \AA}$ . XRD data were recorded on Rigaku smart lab X-ray Diffractometer using monochromatized  $Cu K_{\alpha}$  radiation with Ni filter. X-Ray diffraction at 40 kV was used to estimate the crystallite sizes. The XRD pattern was scanned from 10-80 degrees with the scan rate of  $20 \text{ min}^{-1}$ .

The XRD profile confirmed the hexagonal crystalline nature of the zinc oxide NPs. Intense peaks were obtained at

100,002, 101,102,110, 103 and at 112. The crystal planes are in well accordance with JCPDS No 36-1451 with hexagonal, wurtzite with an average crystalline size of 17.44/15.95.

Debye-Scherrer's equation is  $D = 0.9\lambda/\beta\cos\theta$  where 'D' is crystal size, ' $\lambda$ ' is the wave length of X ray radiation ( $1.5428 \text{ \AA}$ ), ' $\beta$ ' is the full width at half the maximum intensity (FWHM) of diffraction peak and ' $\theta$ ' is the scattering angle. The broadening of the XRD peaks indicates ultrafine nature of the ZnO crystallites.

Diffraction from a crystal is described by Bragg's equation given by  $2d(hkl)\sin\theta = n\lambda$  this equation (1) is used to measure the perpendicular distance (hkl) between imaginary planes, which form parallel families and intersect the repeating unit cell filled with atoms in a way described by the Miller indices (hkl). X-rays of wave length ' $\lambda$ ' may be thought of as reflecting from these imaginary planes at the measurable angle ' $\theta$ ' where ' $n$ ' is the order and ' $\theta$ ' is the diffraction angle. A powder pattern therefore contains a set

of diffraction peaks at ' $2\theta$ ' positions that correspond to the inter plane spacing in the crystal  $D = 0.9\lambda/\beta\cos\theta^{3,7,8,16,28,31}$ .

**SEM studies of ZnO Nanoparticles:** The surface morphology of ZnO nanoparticles was characterised by Goel scanning electron microscope. Figure 4 shows the SEM image of ZnO Nps synthesized by solution combustion method. The particles are agglomerated with irregular morphologies.

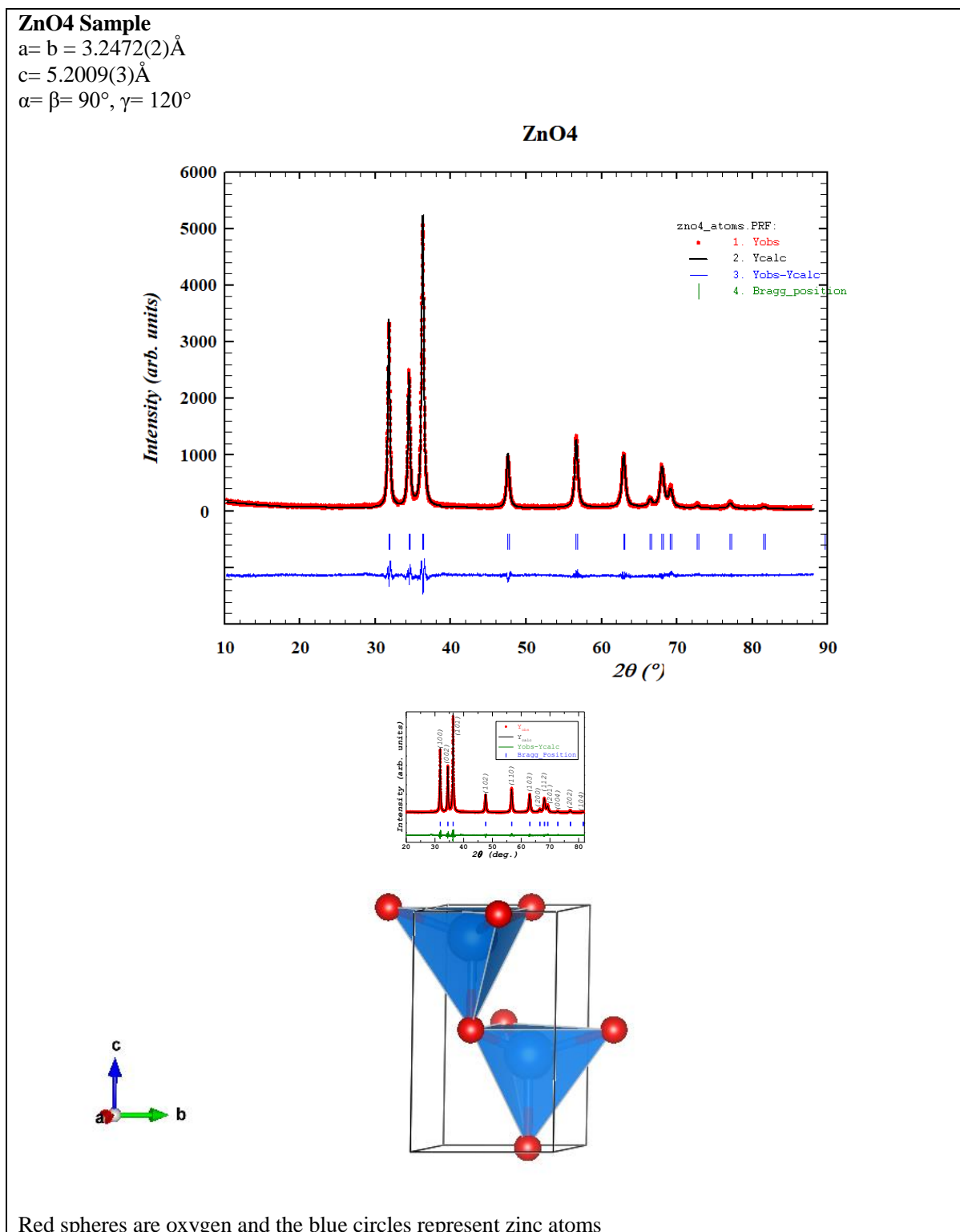


Fig. 3: a, b and c represent the reitveld refinement of ZnO NPs and the arrangement of atoms respectively.

These images demonstrated that zinc oxide nanoparticles are spherical in shape and their sizes are more than the average crystallite size because of the combination of more number of agglomerated particles. SEM images demonstrate that a bulk quantity of flower like bunches exists. Each bunch is gathered of closely packed nanometre scale rods<sup>21</sup>.

**EDAX spectrum:** The 'Zn' and 'O' elemental analysis of the samples was performed by Goel scanning microscope at 25kV with a resolution of 123kV. From the EDAX spectrum, it is confirmed that there is a presence of 'Zn' and 'O'. Further, the absence of other elements in the spectrum indicates the purity of the sample and is shown in fig. 5.

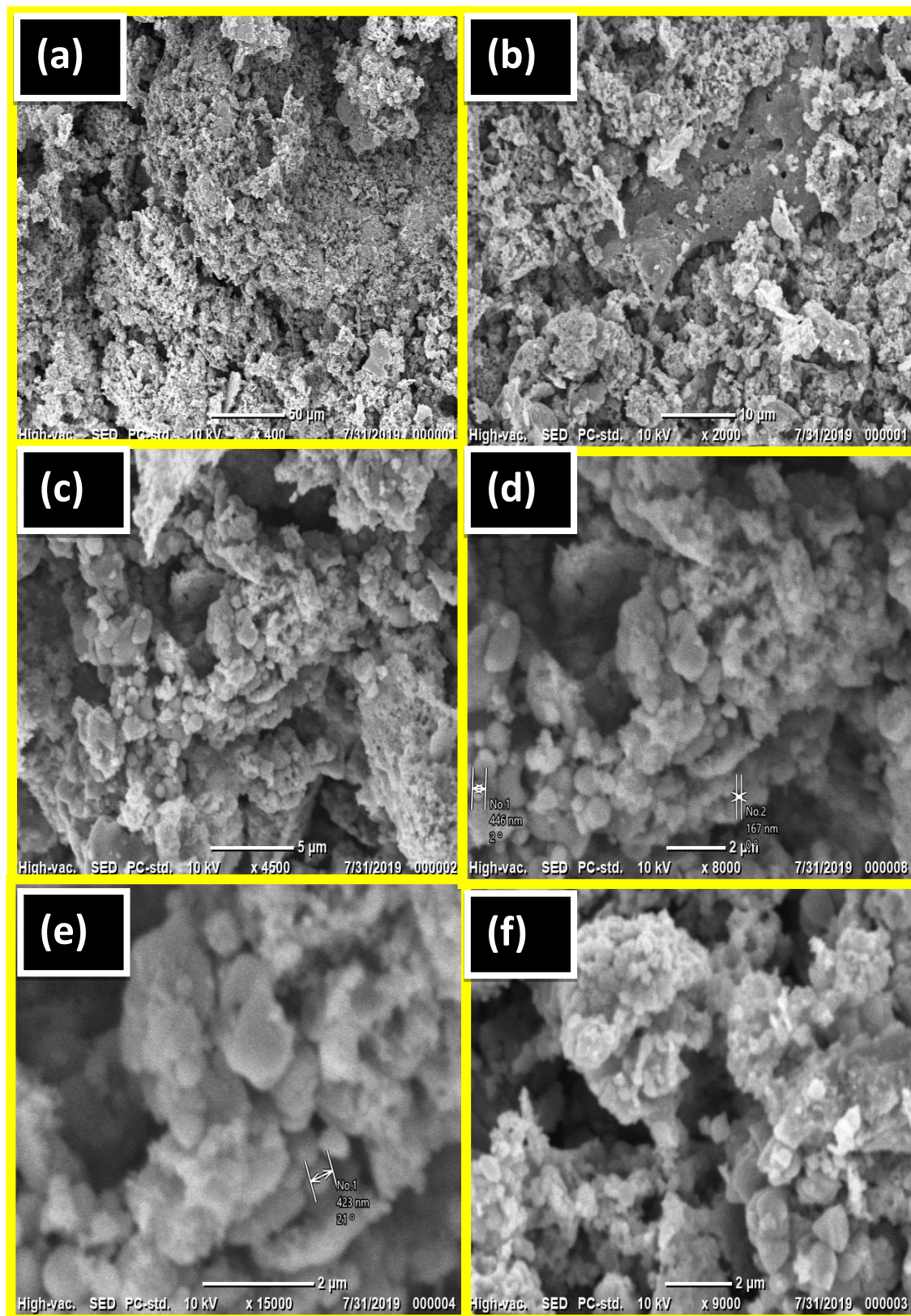


Fig. 4: SEM images of ZnO Nanoparticles

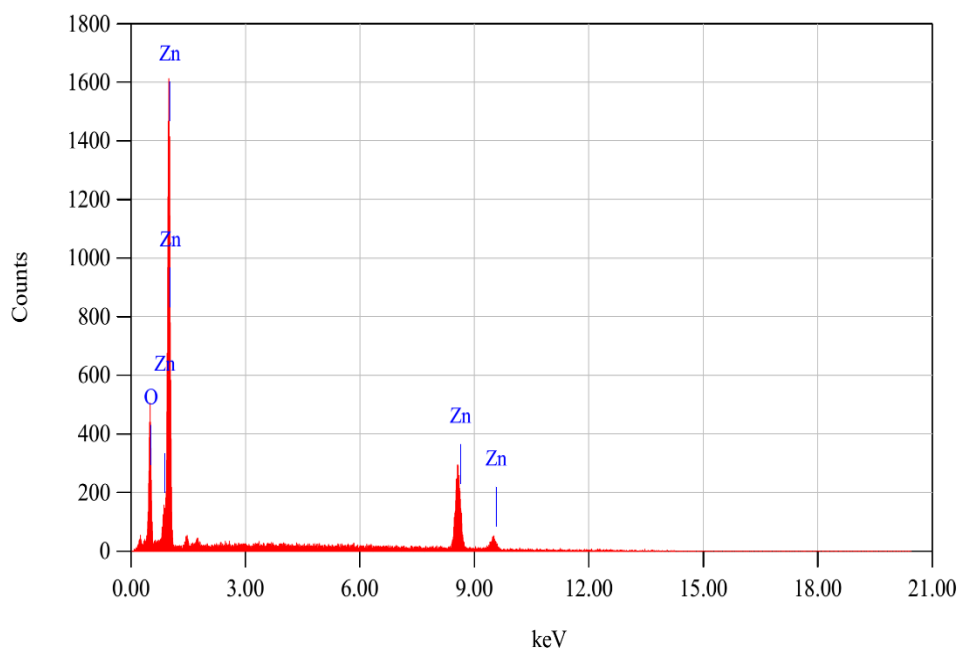


Fig. 5: EDAX spectrum of ZnO Nanoparticles

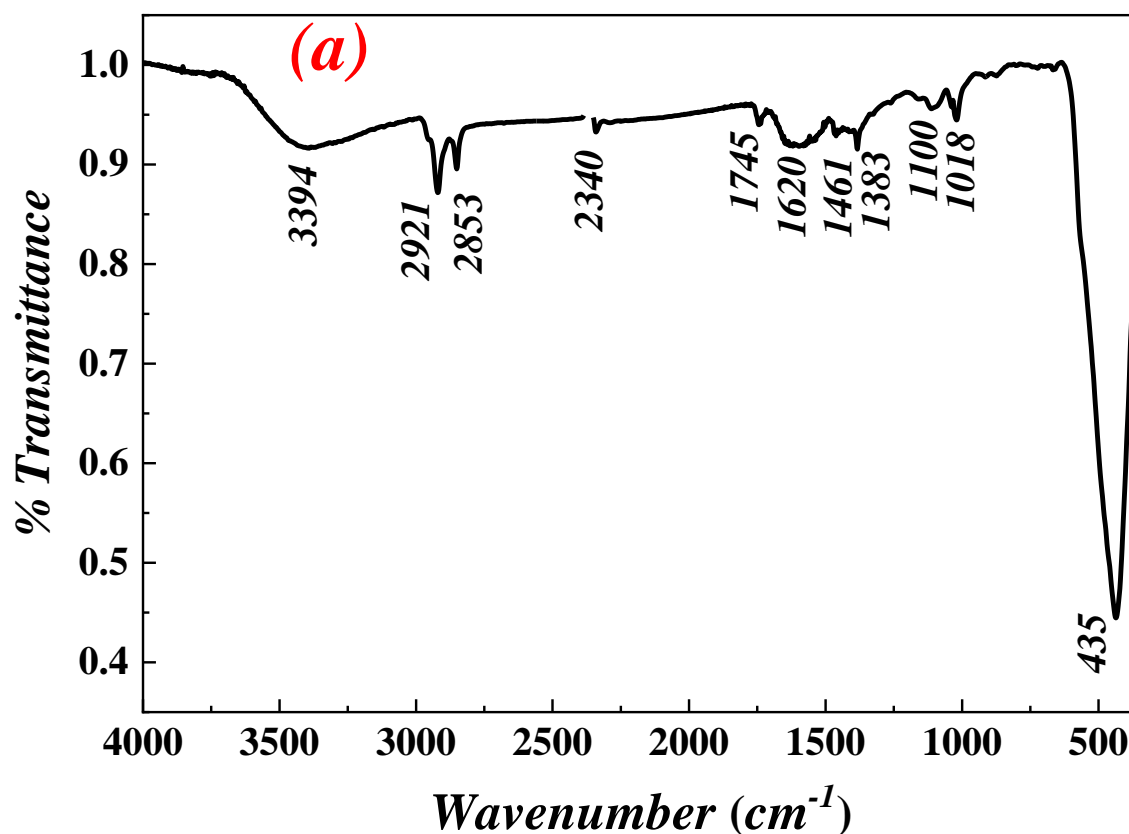


Fig. 6: FTIR Spectrum of ZnO NPS

**FTIR Studies:** *Calophyllum inophyllum* seeds are rich in polypeptidase, proteinase and offer high entropy when they decompose; this entropy is channelized as the fuel in the formation of zinc oxide from zinc nitrate. The purity of the synthesised nanoparticles is addressed in terms of phase purity. The residual components of the fuel are not

quantified in XRD and hence FTIR is better tool for addressing the same. The FTIR spectrum recorded between 400 – 4000  $\text{cm}^{-1}$  is shown in figure 6. The IR spectrum of ZnO nanoparticles shows a broad band at 3394  $\text{cm}^{-1}$  and another band at 1620  $\text{cm}^{-1}$  1620 which are signatures of hydroxyl stretching frequency and bending vibration

corresponding to water. The bands located at 435 can be due to the Zn-O-Zn bending vibration. Peak at  $1018\text{ cm}^{-1}$  is from C-O stretching vibration<sup>13,33</sup>.

**Diffuse Reflectance spectra:** The Kubelka-Munk plots are obtained using the UV-visible diffuse reflectance spectra of ZnONPs shown in figure 7. The reflectance starts to drop around 400 nm for all three samples. Optical bandgap ( $E_g$ ) of these nanoparticles was estimated employing Kubelka-Munk (K-M) model. Initially the  $f(R)$  and the energy are estimated from the following equations:

$$F(R_{\infty}) = \frac{(1-R_{\infty})^2}{2R_{\infty}} \quad (1)$$

and

$$E = h\nu = \frac{hc}{\lambda} \text{ Joules} = \frac{1240}{\lambda} \text{ eV} \quad (2)$$

where  $R_{\infty}$  refers to the reflection coefficient of the sample,  $\lambda$  is the corresponding wavelength. Plot of  $[f(R)*E]^2$  versus energy was plotted as shown in figure 7, the interception of the slope with the x-axis gives the energy of the nanoparticles and value increases from 2.95 to 3.03 eV with decreasing fuel content. These values are in agreement with the expected bandgap of ZnO<sup>2</sup>.

**TEM Studies of ZnO Nanoparticles:** TEM studies of green synthesized ZnO NPs reveal that the particles are connected with each other to form long chain with irregular size as well as shapes as shown in figure 8 (a). However, higher resolution images confirm sphere like particles with size varying between 7 to 9 nm. The spacing between the lines of HRTEM image is around 0.291 nm which corresponds to the 100 orientation of the ZnO crystal as in figure 8 (b). The

electron diffraction image was further analysed using the CrysTBox software<sup>15</sup>. The hkl reflections generated from the image analysis matches with the once expected for the ZnO (Figure 8d). Further diffraction pattern was simulated using the same software and is shown in the inset of the figure 8 (c).

The pattern obtained matches with XRD obtained from the powder diffraction in figure 2 (a). From the electron diffraction ring pattern, it is confirmed that the nanoparticles are polycrystalline in nature with good crystallinity. The agglomeration can be due to the carbon residual which may get coated on to the nanoparticles forming surface layer interconnecting the particles. The carbon coated, however, has dual effect, increase in the photocatalytic activity and reduction in the surface area.

## Results and Discussion

### Evaluation of fuel properties using ZnO NPs and Pumpkin seeds oil:

After completion of transesterification, 82.2% of biodiesel yield was obtained. Further, the fuel properties of biodiesel were evaluated according to ASTM standard. Table 1 shows the fuel properties of biodiesel within the standard limit. Pumpkin oil has high viscosity which is 12-14 times higher than diesel fuel which causes carbon deposition on injector and poor fuel atomization making it difficult to use in diesel engine. By transesterification, viscosity of oil was reduced. Viscosity and density of biodiesel were found to be 5.7cSt and 890 kg/m<sup>3</sup> respectively. Flash point of biodiesel is 176°C which is also in the range of standard and it is safe for transportation and storage. The acid value was found to be 0.25 Mg KOH/g. Therefore, ZnONPs show greater catalytic activity for biodiesel production from pumpkin oil<sup>22</sup>.

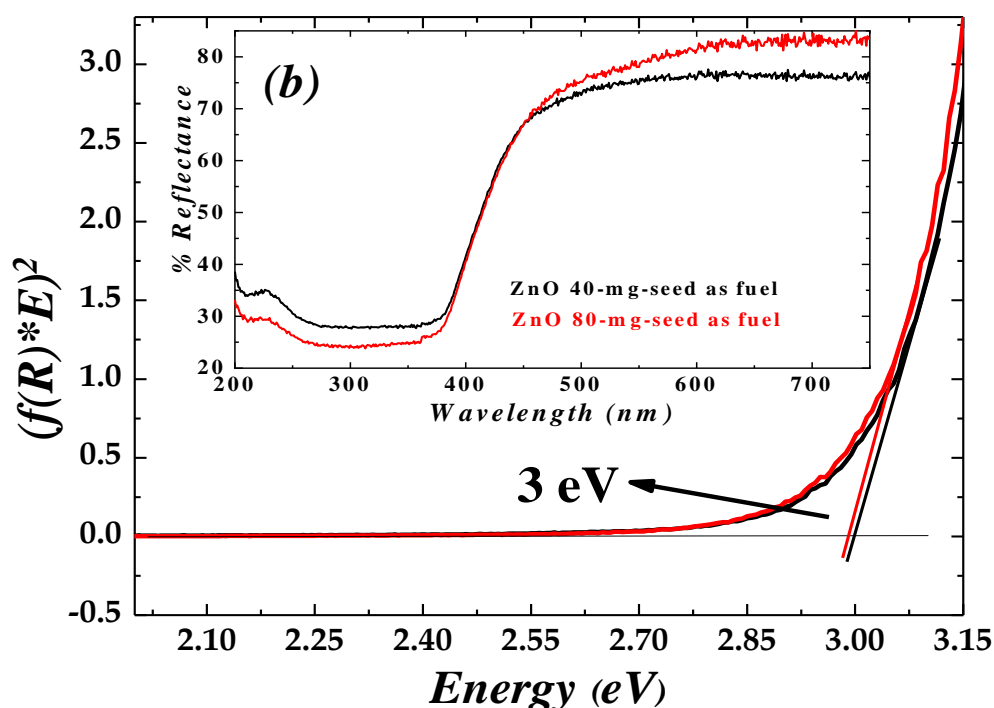


Figure 7: Kubelka Munk plots from Diffuse Reflectance Spectra for the synthesised ceria

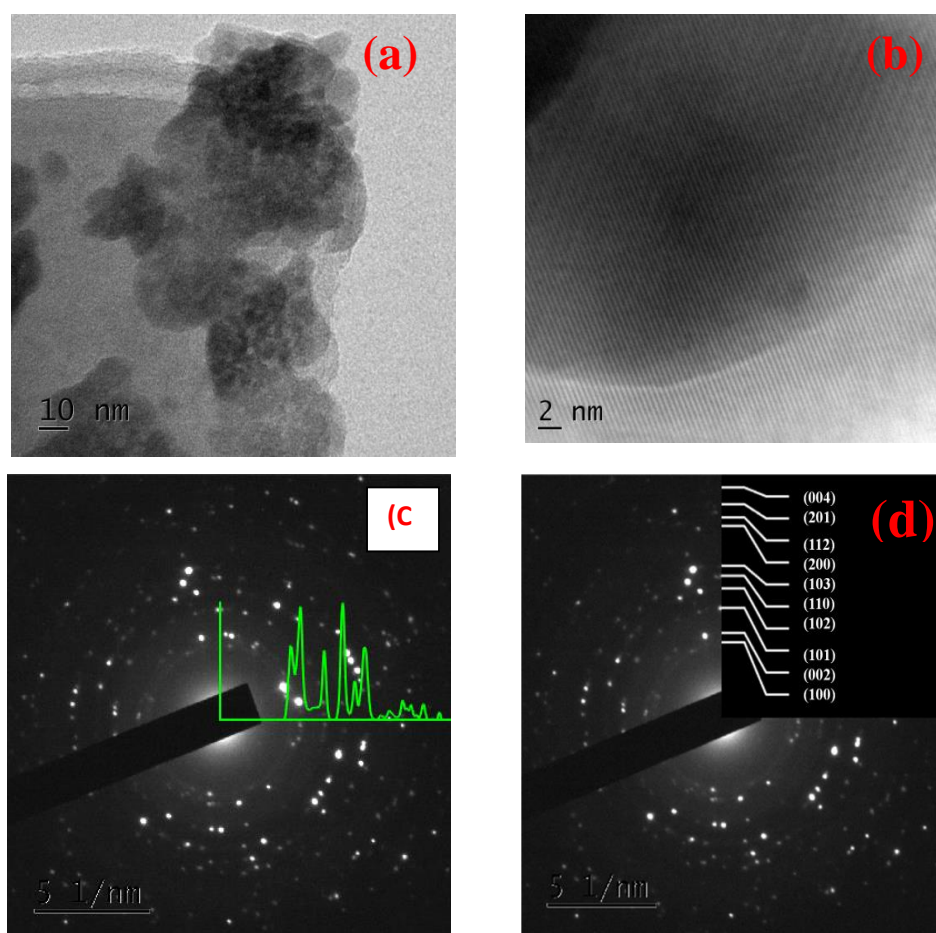


Fig. 8: TEM Images of ZnO NPS

Table 1  
Fuel properties of Biodiesel

Properties	Biodiesel	Diesel	ASTM-6751 Biodiesel
Flash point (°C)	176	60	>130
Density at 15 °C (kg/m <sup>3</sup> )	890	834	-----
Copperstrip corrosion, 50°C, 3h	1a	1a	no. 3 max
Viscosity at 40 °C (cSt)	5.7	2.6	1.9-6.0
Acid value (mg KOH/g)	0.25	0.20	0.50 max
Cloud point	6	-5	-3 to 12

Table 1 shows the various fuel properties of diesel and biodiesel synthesized using the above procedure.

#### Photoluminescence spectra of ZnO Nanoparticles:

Photoluminescence spectra of ZnO nanoparticles were observed using zinc nitrate hexahydrate  $Zn(NO_3)_2 \cdot 6H_2O$ , *Cellophyllum innophyllum* seeds and distilled water by solution combustion method. Well known sharp emission peak at 446nm (near blue emission) due to zinc interstices ( $Zn^{2+}$ ) and Zinc vacancies 487 nm (green emission peak) due to singly ionised oxygen vacancies and surface defects were obtained. Photoluminescence spectra of ZnO nanoparticles emission at 597nm is shown in figure 9b. From the fig. 10, CIE diagram of ZnO NPs was found to be very good emitter of white light and most suitable for use in LED'S<sup>34</sup>.

**Photocatalytic activity of ZnO Nps:** Photocatalytic methylene blue dye degradation was observed with respect to time in the presence of nanometal oxide ZnO.

Synthesized ZnO nanoparticles were used as photo catalyst to examine the degradation of methylene blue under UV source. Aliquot (3mL) was withdrawn after every 30 minutes time intervals from the batch reactor and centrifuged. The degradation percentages calculated as in table 2. The degradation kinetics was studied using the pseudo-first order reaction relation and the rate constant was obtained<sup>10,39</sup>.

**Antibacterial Studies:** The synthesized nanoparticles along with *Escherichia coli*, *Staphylococcus aureus* and *Pseudomonas aeruginosa* were used to determine the ZOI

using the agar disc-diffusion assay<sup>36,37</sup>. The stock solutions of ZnO nanoparticles were prepared by weighing exactly 10 mg and total volume was made up to 10 ml to get 1 mg/ml solution, further it was diluted to get desired concentration in mcg/ml.

Standard ciprofloxacin was also prepared using same protocol. The bacterial cultures were grown in the nutrient broth overnight to attain the ~10<sup>6</sup> (CFU) colony-forming unit /ml. 100 microlitres of each bacteria culture were spread on the agar plates and incubated at 37 °C for 24 hour test and standard studies were also carried out simultaneously. The zone of inhibition was carried out by agar well diffusion method the results are summarized in table 3. Our studies revealed that ceria nanoparticles successfully inhibited the

growth of test organisms with different sized zones of inhibition. Our investigations revealed an encouraging result on the *in vitro* efficacy of ZnO compared to standard drug. The zone of inhibition in mm for the tested organism using two different concentration of ZnO is presented in table 3.

It was observed that ZnO has showed selective anti-microbial activity against the Gram positive organism, whereas Gram negative organism is resistant to all synthesized nanoparticles. From these trials, we confirm good anti-microbial activity of our samples.

**BET surface area:** Figure 12 displays the N<sub>2</sub> Adsorption-Desorption isotherms, it is typical IUPAC type IV pattern with a narrower hysteresis loop, the surface area obtained is 82.09 m<sup>2</sup>/g.

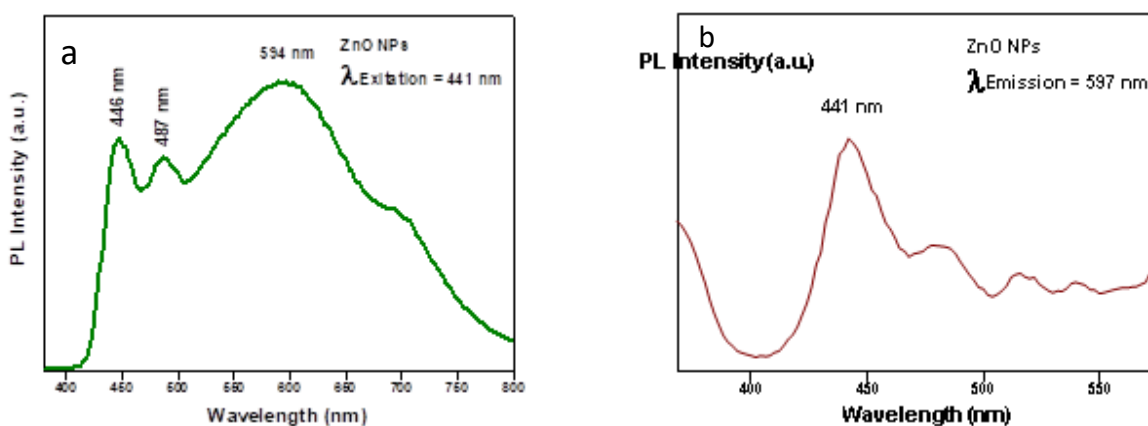


Fig. 9a: Photoluminescence spectra of ZnONanoparticles excited at 441nm.  
 Fig. 9b: Photoluminescence spectra of ZnONanoparticles at emission at 597 nm.  
 (Peaks obtained at 441, 485, 515 and 530 nm)

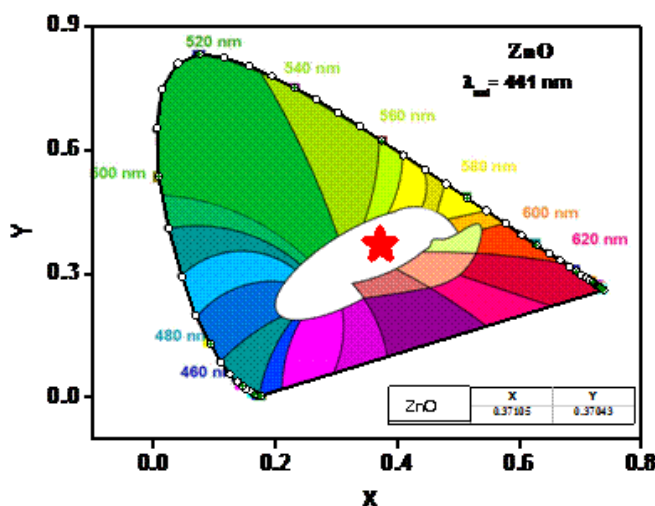


Fig. 10: CIE Diagram of ZnO Nanoparticles synthesized using Zinc nitrate hexahydrate Zn(NO<sub>3</sub>)<sub>2</sub>·6H<sub>2</sub>O, *Celophyllum innophyllum* seed and distilled water by solution combustion method at 500° C

Table 2

Photo catalytic methylene blue dye degradation with respect to time in the presence Nanometal oxide ZnO

S.N.	Nano metal oxide	Time in minutes						
		0.0	30.0	60.0	90.0	120	150	180
1.	ZnO	0.0	18.29	25.8	64.19	91.38	92.30	-----

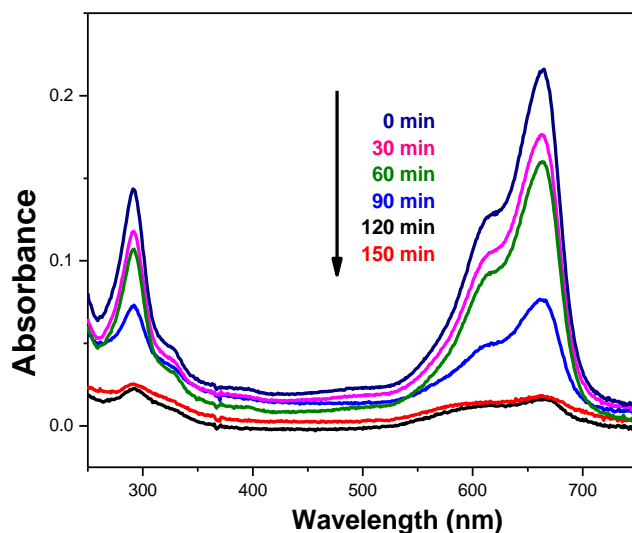


Fig. 11a: UV-Vis spectra of methylene blue dye with respect to different time interval in the presence of ZnO NPs

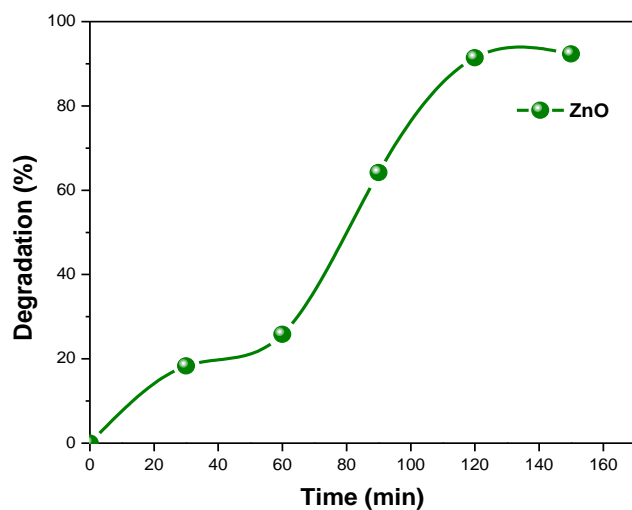


Fig. 11b: Photocatalytic methylene blue dye degradation with respect to time in the presence of ZnO NPs

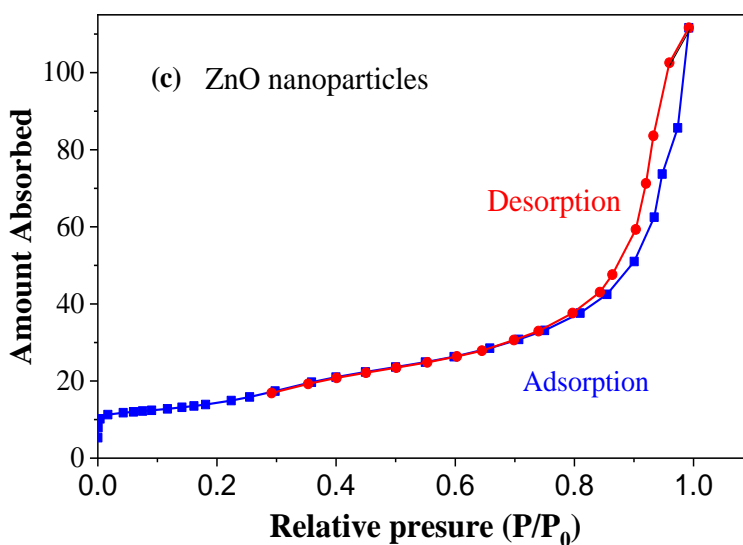


Figure 12: BET N<sub>2</sub> Adsorption-Desorption curves of ZnO Nps

**Table 3**  
**Antibacterial activity of Nanoparticles**

Nanoparticles loading per ml	Zone of Inhibition (mm)		
	<i>Staphylococcus aureus</i>	<i>Pseudomonas aeruginosa</i>	<i>Escherichia coli</i>
ZnO, 100 µg	9±0.25	9±0.19	Not seen
ZnO, 200 µg	11±0.13	10±0.11	Not seen
Ciproflaxacin 10 µg	15±0.09	14±0.08	4±0.15

The pore size of 22 nm was determined from the Barret – Halenda (B-H) pore size distribution plot. The agglomeration of the particles and presence of carbon on the particles may be the reasons for the decreased surface area. The surface area of the zinc oxide nanoparticles can be tuned up to 300 m<sup>2</sup>/g. The presence of the carbon in the grain boundary may result in the interconnection of the grains thereby reducing the total surface area<sup>17,35</sup>.

### Conclusion

ZnO nanoparticles are synthesised using *Calophyllum inophyllum* seed powder as fuel by solution combustion synthesis along with zinc nitrate. The crystallite size can be tuned between 6.5 to 9 nm using appropriate seed concentration, the crystallite size decreases with increasing seed concentration. TEM and FTIR results complement that carbon residue binds the nanoparticles and also helps in increase in the photocatalytic activity. The nanoparticles with surface area of 82.09 m<sup>2</sup>/g showed 93% of photo degradation of methylene blue under UV radiation.

The synthesised zinc oxide nanoparticles were demonstrated as the possible photo catalysts for the conversion of pumpkin oil into biodiesel with a conversion efficiency of around 82%. Thereby, we demonstrate ZnO nanoparticles obtained through combustion synthesis to exhibit excellent photocatalytic activity for biodiesel production.

### References

- Ali B., Yusup S., Quitain A.T., Alnarabiji M.S., Kamil R.N.M. and Kida T., Synthesis of novel graphene oxide/bentonite bifunctional heterogeneous catalyst for one-pot esterification and transesterification reactions, *Energy Convers. Manag.*, **171**, 1801–1812 (2018)
- Anahita Ramesh et al, Photocatalytic activity of ZnO-PbS nanoscale toward Allura Red AC in an aqueous solution: Characterization and mechanism study, *Journal of Photochemistry and Photobiology A: Chemistry*, **434**, 11425 (2023)
- Barrett C.S., Structure of metals, McGraw-Hill Book Company, Inc., New York (1943)
- Barstow M., *Calophyllum inophyllum*, IUCN Red List of Threatened Species, doi:10.2305/IUCN.UK.2019-1.RLTS.T33196A67775081.en, Retrieved 19 November 2021 (2019)
- Borah M.J., Devi A., Borah R. and Deka D., Synthesis and application of Co doped ZnO as heterogeneous nanocatalyst for biodiesel production from non-edible oil, *Renew. Energy*, **133**, 512–519 (2019)

6. *Calophyllum inophyllum* was first described and published in Species Plantarum, *Calophyllum inophyllum*, Germplasm Resources Information Network (GRIN), Agricultural Research Service (ARS), United States Department of Agriculture (USDA) (1753)

7. Chung F.H., Quantitative Interpretation of X-Ray Diffraction Patterns of Mixtures. I. Matrix-Flushing Method for Quantitative Multicomponent Analysis, *Journal of Applied Crystallography*, **7**, 519 (1974)

8. Cullity B.D., Cullity S.R. and Stock S., Elements of X-ray Diffraction, 3<sup>rd</sup> ed. (2001)

9. Höök M. and Tang X., Depletion of fossil fuels and anthropogenic climate change—A review, *Energy Policy*, **52**, 797–809 (2013)

10. Houskova V., Stengl V., Bakardjieva S., Murafa N., Kalendova A. and Oplustil F., Zinc oxide prepared by homogeneous hydrolysis with thioacetamide, its destruction of warfare agents, and photocatalytic activity, *J. Phys. Chem. A*, **111**, 4215 (2007)

11. Jamil F. et al, Heterogeneous carbon-based catalyst modified by alkaline earth metal oxides for biodiesel production: Parametric and kinetic study, *Energy Convers. Manag.*, **10**, 100047 (2021)

12. Jume B.H., Gabris M.A., Nodeh H.R., Rezanian S. and Cho J., Biodiesel production from waste cooking oil using a novel heterogeneous catalyst based on graphene oxide doped metal oxide nanoparticles, *Renew. Energy*, **162**, 2182–2189 (2020)

13. Kannadasan N. et al, Optical behavior and sensor activity of Pb ions incorporated ZnO nanocrystals, *Spectrochimica Acta Part A: Molecular and Biomolecular Spectroscopy*, **143**, 179 (2015)

14. Kavalli K., Hebbar G.S., Shubha J.P., Adil S.F., Khan M., Hatshan M.R., Almutairi A.M. and Shaik B., Green Synthesized ZnO Nanoparticles as Biodiesel Blends and their Effect on the Performance and Emission of Greenhouse Gases, *Molecules*, **27**, 2845, <https://doi.org/10.3390/molecules27092845> (2022)

15. Klinger M. and Jäger A., Crystallographic Tool Box (CrysTBox): automated tools for transmission electron microscopists and crystallographers, *J Appl Crystallogr.*, doi:10.1107/S1600576715017252 (2015)

16. Kumar P. et al, Investigations on structural, optical and second harmonic generation in solvothermally synthesized pure and Cr-doped ZnO nanoparticles, *Cryst Eng Comm*, **14**, 1653–1658 (2012)

17. Kuśnieruk S. et al, Influence of hydrothermal synthesis parameters on the properties of hydroxyapatite nanoparticles, *Beilstein Journal of Nanotechnology*, **7**, 1586 (2016)

18. Madhuvilakku R. and Piraman S., Biodiesel synthesis by TiO<sub>2</sub>-ZnO mixed oxide nanocatalyst catalyzed palm oil transesterification process, *Bioresour. Technol.*, **150**, 55–59 (2013)
19. Manchali S., Chidambara Murthy K.N., Vishnuvardana and Patil B.S., Nutritional Composition and Health Benefits of Various Botanical Types of Melon (*Cucumis melo* L.), *Plants*, **10**, 1755, <https://doi.org/10.3390/plants10091755> (2021)
20. Marulasiddeshwara M.B., Dakshayani S.S., Sharath Kumar M.N., Chethana R., Raghavendra Kumar P. and Devaraja S., Facile-one pot-green synthesis, antibacterial, antifungal, antioxidant and antiplatelet activities of lignin capped silver nanoparticles: A promising therapeutic agent, *Mater Sci Eng C Mater Biol Appl.*, **81**, 182-180 (2017)
21. Menaka Priya Balaji and Devi Rajeswari V., Endothelial Dysfunction associated with Diabetes Mellitus linked to extracellular signal-regulated kinase and inflammatory pathways, *Res. J. Biotech.*, **18(1)**, 135-146 (2022)
22. Nanda Saridewi, Adelian Risa Adinda and Siti Nurbayti, Characterization and Antibacterial Activity Test of Green Synthetic ZnO Nanoparticles Using Avocado (*Persea americana*) Seed Extract, *Jurnal Kimia Sains dan Aplikasi*, **25(3)**, 116-122 (2022)
23. Naveed Ul Haq A., Nadhman A., Ullah I., Mustafa G., Yasinzaï M. and Khan I., Synthesis approaches of zinc oxide nanoparticles: The dilemma of ecotoxicity, *J. Nanomater.*, **2017**, 8510342 (2017)
24. Netravathi P.C. and Suresh D., Silver-doped ZnO embedded reduced graphene oxide hybrid nanostructured composites for superior photocatalytic hydrogen generation, dye degradation, nitrite sensing and antioxidant activities, *Inorganic Chemistry Communications*, **134**, 109051 (2021)
25. Othman M.F., Adam A., Najafi G. and Mamat R., Green fuel as alternative fuel for diesel engine: A review, *Renew. Sust. Energy Rev.*, **80**, 694–709 (2017)
26. Quirino M.R., Oliveira M.J.C., Keyson D., Lucena G.L., Oliveira J.B.L. and Gama L., Synthesis of zinc oxide by microwavehydrothermal method for application to transesterification of soybean oil (biodiesel), *Mater. Chem. Phys.*, **185**, 24–30 (2017)
27. Rai H.S., Bhattacharyya M.S., Singh J., Bansal T.K., Vats P. and Banerjee U.C., Removal of dyes from the effluent of textile and dyestuff manufacturing industry: a review of emerging techniques with reference to biological treatment, *Crit. Rev. Environ. Sci. Technol.*, **35(3)**, 219-238 (2005)
28. Raoufi D. and Raoufi T., The effect of heat treatment on the physical properties of sol-gel derived ZnO thin films, *Applied Surface Science*, **255**, 5812 (2009)
- 28a. Rudreshappa G.E., Chennabasappa Madhu, Sreenivasa S., Vijaya Kumar S. and Aruna Kumar D.B., Green Synthesis of Cerium Oxide Nanoparticles, Antibacterial Studies and as Catalyst for the Conversion of Cotton Seed Oil into Biodiesel, *Asian Journal of Chemistry*, <https://doi.org/10.14233/ajchem.2022.23607> (2022)
29. Saira Sehar et al, Synthesis of Zinc Oxide Nano particles from Moringa Tree leaves by Green Method and also check its Antibacterial activity against Gram Positive and Gram Negative Bacteria, *Asian Journal of Pharmacy and Technology*, **12(3)**, 213-7 (2022)
30. Seetawan U. et al, Effect of calcinations temperature on crystallography and nanoparticles in ZnO disk, *Materials Sciences and Applications*, **2**, 1302 (2011)
31. Shafiee S. and Topal E., When will fossil fuel reserves be diminished?, *Energy Policy*, **37**, 181–189 (2009)
32. Shi L. and Gunasekaran S., *Nanoscale Research Letters*, **3**, 491 (2008)
33. Sikdar Bratati, Raj Adarsha and Roy Sudipta, Exploration of antibacterial and antioxidant potential of a few members of the family Piperaceae, *Res. J. Biotech.*, **17(8)**, 59-69 (2022)
34. Sivakami R., Dhanuskodi S. and Karvembu R., Estimation of lattice strain in nanocrystalline RuO<sub>2</sub> by Williamson–Hall and size–strain plot methods, *Spectrochimica Acta Part A: Molecular and Biomolecular Spectroscopy*, **152**, 43 (2016)
35. Taiba Naseem and Tayyiba Durrani, The role of some important metal oxide nanoparticles for wastewater and antibacterial applications: A review, *Environmental Chemistry and Ecotoxicology*, **3**, 59-75 (2021)
36. Thiruppathi C., Kumaravel P., Duraisamy R., Prabhakaran A.K., Jeyanthi T., Sivaperumal R. and Karthick P.A., Biofabrication of Silver nanoparticles using *Cocculus hirsutus* leaf extract and their antimicrobial efficacy. Silver nanoparticles, *Cocculus hirsutus*, Antimicrobial activity, *Asian J. Pharm. Tech.*, **3(3)**, 93-97 (2013)
37. Wang A., Quan W., Zhang H., Li H. and Yang S., Heterogeneous ZnO-containing catalysts for efficient biodiesel production, *RSC Adv.*, **11**, 20465–20478 (2021)
38. Xu F., Zhang P., Navrotsky A., Yuan Z.Y., Ren T.Z., Halasa M. and Su B.L., Hierarchically Assembled Porous ZnO Nanoparticles: Synthesis, Surface Energy, and Photocatalytic Activity, *Chem. Mater.*, **19**, 5680 (2007)
39. Yoo S.J., Lee H.S., Veriansyah B., Kim J., Kim J.D. and Lee Y.W., Synthesis of biodiesel from rapeseed oil using supercritical methanol with metal oxide catalysts, *Bioresour. Technol.*, **101**, 8686–8689 (2010)
40. Zak A.K., Abrishami M.E., Majid W.H.A., Yousefi R. and Hosseini S.M., Effects of annealing temperature on some structural and optical properties of ZnO nanoparticles prepared by a modified sol–gel combustion method, *Ceram. Int.*, **37**, 393–398 (2011).

(Received 29<sup>th</sup> November 2022, accepted 27<sup>th</sup> January 2023)